

# Addressing $H_0$ tension by means of VCDM

Antonio De Felice,<sup>1,\*</sup> Shinji Mukohyama,<sup>1,2,†</sup> and Masroor C. Pookkillath<sup>1,‡</sup>

<sup>1</sup>*Center for Gravitational Physics, Yukawa Institute for Theoretical Physics, Kyoto University, 606-8502, Kyoto, Japan*

<sup>2</sup>*Kavli Institute for the Physics and Mathematics of the Universe (WPI),  
The University of Tokyo, Kashiwa, Chiba 277-8583, Japan*

Tensions in quantifying the present expansion rate of the universe,  $H_0$ , from the high-redshift observation and low-redshift observations have been growing during these past few years. This is one of the most surprising and hardest challenges that the present day cosmology needs to face. These experimental results are difficult to accept as they immediately challenge the standard model of cosmology known as the  $\Lambda$  Cold Dark Matter ( $\Lambda$ CDM) model. On the other hand, once the experimental results are accepted, we need to face the possibility that the choice of this model is nothing but an arbitrarily chosen theoretical prior in the estimation of the cosmological parameters of the universe (including  $H_0$ ). Here we show that the  $H_0$ -tensions can be resolved by changing the theoretical prior on using a new theory, dubbed VCDM. This is essentially a low-redshift resolution of the Hubble tension.

The value of today's rate of expansion of the universe,  $H_0$ , has been measured, as a direct measurement, from low-redshift observations, namely, Hubble Space Telescope [1] (HST), H0LiCOW [2], Megamaser Project [3] (MCP) and Carnegie-Chicago Hubble Program (CCHP) Collaboration [4]. Among these observations HST in particular has achieved a remarkable precision providing  $H_0 = 74.03 \pm 1.42$ . On the other hand, on assuming some theoretical model,  $H_0$  can also be deduced from the measurement of temperature power spectra in the Cosmic Microwave Background Radiation (CMB) which is produced at the recombination time. The recent Planck Legacy 2018 release gives  $H_0 = 67.04 \pm 0.5$ , assuming the standard flat- $\Lambda$ CDM model (non-flat versions are known to be strongly disfavored by other data, e.g. Baryon Acoustic Oscillations (BAO)) [5]. Hence, the tension between this theoretical model and experimental results adds up to more than  $4\sigma$ 's [6, 7].

However, the flat- $\Lambda$ CDM could be representing only a first approximation to another, improved model of our universe. The VCDM theory, described in the following, was originally introduced for the purpose of seeking minimal theoretical deviations from the standard model of gravity and cosmology, i.e. General Relativity (GR) and  $\Lambda$ CDM, as it does not introduce any new physical degrees of freedom, but on the other hand, one can have, as we will show in the following, a non-trivial and interesting phenomenology.

The VCDM theory [8], in which the cosmological constant  $\Lambda$  in the standard  $\Lambda$ CDM is promoted to a function  $V(\phi)$  of a non-dynamical, auxiliary field  $\phi$  without introducing extra physical degrees of freedom. This theory of modified gravity breaks four dimensional diffeomorphism invariance at cosmological scales but keeps the three dimensional spatial diffeomorphism invariance. On doing so, the theory modifies gravity at cosmological scales while it only possess two gravitational degrees of freedom as in GR. In general this allows a spectrum of possibilities typically much larger than the case of a scalar-tensor

theory. For the latter, the extra scalar degree of freedom is not only strongly bound on solar system scales (for which one needs the scalar to be very massive or to be shielded by some non-trivial dynamical mechanisms, e.g. chameleon or Vainshtein), but also on cosmological scales (for which one needs to constrain the background dynamics as to avoid ghost and gradient instabilities).

The equations of motion for the VCDM theory on a homogeneous and isotropic background can be written as

$$V = \frac{1}{3}\phi^2 - \frac{\rho}{M_{\text{P}}^2}, \quad \frac{d\phi}{d\mathcal{N}} = \frac{3}{2} \frac{\rho + P}{M_{\text{P}}^2 H}, \quad \frac{d\rho_i}{d\mathcal{N}} - 3(\rho_i + P_i) = 0, \quad (1)$$

where  $\mathcal{N} = \ln(a/a_0)$  ( $a$  being the scale factor and  $a_0$  being its present value),  $H = \dot{a}/a^2$  is the Hubble expansion rate (a dot denotes differentiation with respect to the conformal time),  $\rho = \sum_i \rho_i$  and  $P = \sum_i P_i$  (the sum is over the standard matter species). Unless  $\rho + P = 0$ , the following equation follows from the above equations:  $\phi = \frac{3}{2}V_{,\phi} - 3H$ . When  $V$  is a linear function of  $\phi$ , as in  $V = \lambda_1\phi + \lambda_0$ , then the equations of motion (1) reduce to

$$3H^2 = \frac{\rho}{M_{\text{P}}^2} + \Lambda, \quad H \frac{dH}{d\mathcal{N}} = -\frac{\rho + P}{2M_{\text{P}}^2}, \quad \frac{d\rho_i}{d\mathcal{N}} - 3(\rho_i + P_i) = 0, \quad (2)$$

where  $\Lambda \equiv \lambda_0 + 3\lambda_1^2/4 = \text{const}$ . These are nothing but the equations of motion in the standard  $\Lambda$ CDM model. Hence, the VCDM theory extends the  $\Lambda$ CDM model by replacing the constant  $\Lambda$  with a free function  $V(\phi)$ . Yet, the VCDM theory does not introduce extra degrees of freedom in the sense that the number of independent initial conditions is the same as  $\Lambda$ CDM. The ‘‘V’’ of VCDM therefore stands for the free function  $V(\phi)$  introduced in this theory.

In the following we want to be able to use the free function  $V(\phi)$  in order to give any wanted background evolution for  $H$  which can be given as  $H = H(\mathcal{N})$ . From the 2nd of (1), having given  $H$  as a function of  $\mathcal{N}$ , then

one obtains

$$\phi(\mathcal{N}) = \phi_0 + \int_{\mathcal{N}_0}^{\mathcal{N}} \frac{3}{2} \frac{\rho(\mathcal{N}') + P(\mathcal{N}')}{M_{\text{Pl}}^2 H(\mathcal{N}')} d\mathcal{N}', \quad (3)$$

where  $\phi_0 = \phi(\mathcal{N}_0)$ . Assuming that  $\rho + P > 0$ , and  $H > 0$ , the right hand side of (3) is an increasing function of  $\mathcal{N}$  and thus the function  $\phi(\mathcal{N})$  has a unique inverse function,  $\mathcal{N} = \mathcal{N}(\phi)$ . Obviously,  $\mathcal{N}$  is an increasing function of  $\phi$ . By combining this with the 1st of (1), one obtains

$$V(\phi) = \frac{1}{3} \phi^2 - \frac{\rho(\mathcal{N}(\phi))}{M_{\text{Pl}}^2}. \quad (4)$$

Therefore we have obtained a simple and powerful reconstruction mechanism for  $V$  for a given and wanted evolution of  $H$ . Once  $V(\phi)$  is specified in this way, we know how to evolve not only the homogeneous and isotropic background but also perturbations around it.

We now introduce two choices of  $H(z)$  to address current cosmological tensions: one in the flat- $\Lambda$ CDM and

the other in the VCDM. The former is  $H_\Lambda^2 \equiv H_{\Lambda 0}^2 [\tilde{\Omega}_\Lambda + \tilde{\Omega}_{m0}(1+z)^3 + \tilde{\Omega}_{r0}(1+z)^4]$ , where  $\tilde{\Omega}_\Lambda \equiv 1 - \tilde{\Omega}_{m0} - \tilde{\Omega}_{r0}$ , and the latter is

$$H^2 = H_\Lambda^2 + A_1 H_0^2 \left[ 1 - \tanh\left(\frac{z - A_2}{A_3}\right) \right], \quad (5)$$

with the idea that  $0 < A_2 < 2$ . In this case we have at early times, for  $z \gg |A_2|$ , that the system will tend to be the standard flat- $\Lambda$ CDM evolution, i.e.  $H^2 \approx H_\Lambda^2$ . Today, i.e. for  $z = 0$ , we have  $H_0^2 = H_\Lambda^2 + A_1 H_0^2 \left[ 1 + \tanh\left(\frac{A_2}{A_3}\right) \right]$ , which can be solved today for  $A_1$ , to give  $A_1 = \frac{H_0^2 - H_\Lambda^2}{H_0^2 \left[ \tanh\left(\frac{A_2}{A_3}\right) + 1 \right]}$ .

Let us further consider the following parameter redefinitions  $\tilde{\Omega}_{m0} = \Omega_{m0} \frac{H_0^2}{H_{\Lambda 0}^2}$ ,  $\tilde{\Omega}_{r0} = \Omega_{r0} \frac{H_0^2}{H_{\Lambda 0}^2}$ , and  $\beta_H = \frac{H_{\Lambda 0}}{H_0}$ , then we find

$$\frac{H^2}{H_0^2} = \Omega_{m0}(1+z)^3 + \Omega_{r0}(1+z)^4 + (1 - \beta_H^2) \frac{1 + \tanh\left(\frac{A_2 - z}{A_3}\right)}{1 + \tanh\left(\frac{A_2}{A_3}\right)} + \beta_H^2 \left( 1 - \frac{\Omega_{m0}}{\beta_H^2} - \frac{\Omega_{r0}}{\beta_H^2} \right). \quad (6)$$

So in total we have six background parameters (three more than  $\Lambda$ CDM). However, we can reduce them to five (two more than  $\Lambda$ CDM) by fixing  $A_3$  as we expect to have a large degeneracy (after assuming  $A_2 \sim 1$ ). According to Akaike Information Criterion (AIC), we can accept the model if we can have an improvement of  $\chi^2$  larger than four in comparison with  $\Lambda$ CDM [9]. In fact, we will show later on that the  $\chi^2$  has improved remarkably by 20.60 with respect to  $\Lambda$ CDM. In particular, we will fix, later on,  $A_3$  to the value of  $10^{-3}$ .

Two things need to be noticed. First, having given the expression for  $H = H(z)$ , one automatically can deduce all the needed background expressions. Second, the fact we have an MMG-component does not mean we are adding a physical dark-component degree of freedom. In fact, for this theory, there is no additional physical degree of freedom, beside the tensorial gravitational waves and the standard ones related to the presence of matter

fields [8].

After having introduced the behavior of the VCDM model on a FLRW background, we will test it against several cosmological data to see how well it can address the  $H_0$  tension. Here we use Planck Legacy 2018 data with `planck_highl_TTEEE`, `planck_lowl_EE`, and `planck_lowl_TT` [10], baryon acoustic oscillation (BAO) from 6dF Galaxy Survey [11] and the Sloan Digital Sky Survey [12, 13], Joint light Analysis (JLA) comprised of 740 type Ia supernovae [14], and SH0ES consisting of a single data point [1]  $H_0 = 74.03 \pm 1.42$ .

Both the background and linear perturbation equations of motion are implemented in the Boltzmann code CLASS [15], with covariantly corrected baryon equations of motion [16].

For a matter action at second order up to shear for a fluid we proceed here by first writing the Schutz-Sorkin Lagrangian (SSL) for a single fluid [16], as follows

$$S_{\text{SSL}} = - \int d^4x \sqrt{-g} [\rho(n, s) + J^\mu (\partial_\mu \ell + \theta \partial_\mu s + A_1 \partial_\mu B_1 + A_2 \partial_\mu B_2)], \quad (7)$$

with  $n = \sqrt{-J^\mu J^\mu g_{\mu\nu}}$ , and 4-velocity  $u^\alpha = J^\alpha/n$ . We consider several copies of the previous action each

describing a different fluid, labeled with an index  $I$ . Then we can expand the previous SSL up to second

order in the perturbation fields, and to this one, we then add a correction aimed to describe an anisotropic fluid as follows  $S_m^{(2)} = S_{\text{SSL}}^{(2)} + S_{\text{corr}}^{(2)}$ , where  $S_{\text{corr}}^{(2)} = \int dt d^3x N a^3 \sum_I \sigma_I \Theta_I$  and  $\Theta_I$  stands for a linear combination of perturbation fields. Since for each matter species  $\rho_I = \rho_I(n_I)$ , and  $n_I = \sqrt{-J_I^\mu J_I^\nu g_{\mu\nu}}$ , one can find a relation among  $\delta\rho_I$  and the other fields as  $\delta J_I = \frac{\rho_I}{n_I \rho_{I,n}} \frac{\delta\rho_I}{\rho_I} - \alpha$ , where  $\delta N = N(t)\alpha$ , which can be used as a field redefinition to replace  $\delta J_I$  in terms of  $\frac{\delta\rho_I}{\rho_I}$ . We also define gauge invariant combinations  $v_I = -\frac{\rho_I}{k^2} \theta_I + \chi - \frac{a^2}{N} \partial_t(E/a^2)$ ,  $\alpha = \psi - \frac{\dot{\chi}}{N} + N^{-1} \partial_t[a^2 N^{-1} \partial_t(E/a^2)]$ , and  $\zeta = -\phi - H\chi + \frac{a^2 H}{N} \partial_t(E/a^2)$ , where  $\delta\gamma_{ij} = 2[a^2 \zeta \delta_{ij} + \partial_i \partial_j E]$ , and  $\delta u_{Ii} = \partial_i v_I$ . We find finally that

$$S_{\text{corr}}^{(2)} = \int dt d^3x N a^3 \sum_I \sigma_I [\delta\rho_I + 3(\rho_I + P_I)\zeta]. \quad (8)$$

$$\begin{aligned} \mathcal{L} = N a^3 \delta^{ij} \left\{ \sum_I n_I \rho_{I,n} \frac{\dot{F}_i^I}{N} \delta u_j^I + \frac{1}{a^2} \sum_I n_I \rho_{I,n} \left[ a \delta u_i^I V_j - \frac{1}{2} \delta u_i^I \delta u_j^I \right] - \frac{M_{\text{P}}^2}{4a^2} V_i (\delta^{lm} \partial_l \partial_m V_j) \right. \\ \left. - \frac{1}{2a^2} \sum_I p_I \pi_i^{I,T} (\delta^{lm} \partial_l \partial_m F_j^I) \right\}, \end{aligned} \quad (9)$$

which reduces to the same result as in GR.

Finally, for the tensor modes, let us define  $\delta\gamma_{ij} = a^2 (h_+ \varepsilon_{ij}^+ + h_\times \varepsilon_{ij}^\times)$ , where  $\varepsilon_{ij}^{+,\times} = \varepsilon_{ji}^{+,\times}$ ,  $\delta^{ij} \varepsilon_{ij}^{+,\times} = 0$ ,  $\varepsilon_{ij}^+ \varepsilon_{mn}^\times \delta^{im} \delta^{jn} = 0$ , and  $\varepsilon_{ij}^+ \varepsilon_{mn}^+ \delta^{im} \delta^{jn} = 1 =$

$$\mathcal{L} = \frac{M_{\text{P}}^2}{8} \frac{a^3}{N} (\dot{h}_+^2 + \dot{h}_\times^2) - \frac{N a M_{\text{P}}^2}{8} [(\partial_i h_+) \delta^{ij} (\partial_j h_+) + (\partial_i h_\times) \delta^{ij} (\partial_j h_\times)] + \frac{N a}{2} \sum_I p_I (h_+ \pi_+^I + h_\times \pi_\times^I), \quad (10)$$

which reduces to the same form of GR.

All the equations of motion (including the ones for the matter fields) for the perturbations are, in form, exactly the same as for  $\Lambda$ CDM (the only difference being the explicit dependence of  $H$  on the redshift), except the following one, which is written in terms of the Newtonian-gauge invariant fields  $\phi$  and  $\psi$ :

$$\dot{\phi} + aH\psi = \frac{3[k^2 - 3a^2(\dot{H}/a)]}{k^2 [2k^2/a^2 + 9\sum_j (\varrho_j + p_j)]} \sum_i (\varrho_i + p_i) \theta_i, \quad (11)$$

which is used to find the evolution of the curvature perturbation  $\phi$ , and where a dot represents a derivative with respect the conformal time.

The parameter estimation is made via Markov chain Monte Carlo (MCMC) sampling by using Monte Python [17, 18] against the above mentioned data sets.

For vector transverse modes, we can define  $T_{Ij}^i \equiv p_I \delta^i_j + p_I \frac{\delta^{ik}}{a^2} \pi_{kj}^I$ , and  $\pi_{ij}^I \equiv \frac{1}{2} (\partial_i \pi_j^{I,T} + \partial_j \pi_i^{I,T})$ . Then we can introduce the 1+3 decompositions for the 4-velocity of the fluid  $u_{Ii}^{V,I} = \delta u_{Ii}^I$ , the shift  $N_i = a N G_i$ , and the 3D metric  $\delta\gamma_{ij} = a(\partial_i C_j + \partial_j C_i)$ . We can also introduce the following gauge invariant variables  $V_i = G_i - \frac{a}{N} \frac{d}{dt} \left( \frac{C_i}{a} \right)$ , and  $F_i^I = \frac{C_i}{a} - \frac{b_{1i}^I}{b_1^I \cdot b_1^I} \delta B_1^I - \frac{b_{2i}^I}{b_2^I \cdot b_2^I} \delta B_2^I$ , where  $b_{1i}^I b_{2i}^I = 0 = b_{1i}^I k^i = b_{2i}^I k^i$ . Then, on following a similar approach one finds the total Lagrangian density for the vector perturbations, in VCDM, can be written as

$\varepsilon_{ij}^\times \varepsilon_{mn}^\times \delta^{im} \delta^{jn}$ . As for the energy-momentum tensor we have instead for the perturbations  $\delta T_{Ij}^i \equiv p_I \frac{\delta^{ik}}{a^2} \pi_{kj}^{I,TT}$ , so that the total Lagrangian density in MMG becomes

The analysis of the MCMC chains is performed using a chain analyzer package, GetDist [19].

We have considered the prior for the parameters of VCDM such that  $\Lambda$ CDM is well inside the region. In particular, we give  $0.6 < \beta_H < 2.3$ , and  $-0.5 < A_2 < 3$ , fixing  $A_3 = 10^{-3}$  as it has large degeneracy. Deviations of  $\beta_H$  from 1 imply that the cosmological data sets prefer the VCDM model over  $\Lambda$ CDM.

After doing the chain analysis we found a remarkable improvement in the fitness parameter with respect to that of  $\Lambda$ CDM,  $\Delta\chi^2 = 20.60$ . Also we found that the value of  $H_0$  from VCDM after the parameter estimation is in full agreement with the low redshift measurement,  $H_0 = 73.9_{-2.7}^{+2.7}$ . Hence, the  $H_0$  tension is unravelled within this model.

In order to have a better picture of the  $\chi^2$  for cosmological data sets, in Table I we compare effective  $\chi^2$  of

Experiments	VCDM	$\Lambda$ CDM
Planck_high_TTTEEE	2346.36	2351.98
Planck_lowl_EE	396.01	396.74
Planck_lowl_TT	23.00	22.39
JLA	682.00	683.07
bao_boss_dr12	3.81	3.65
bao_smallz_2014	1.48	2.41
hst	$1.3 \times 10^{-3}$	13.03
Total	3452.67	3473.27

Table I. Comparison of effective  $\chi^2$  between VCDM and  $\Lambda$ CDM for individual data sets.

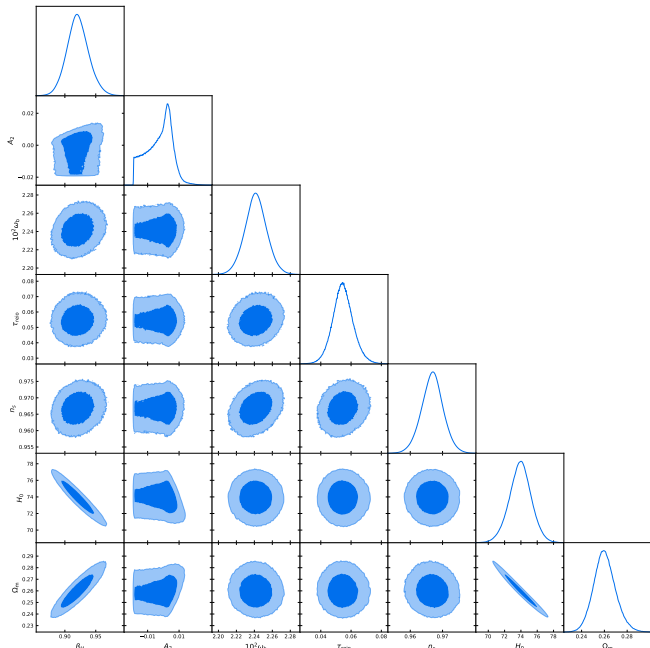


Figure 1. 2-dimensional marginalised likelihoods for the VCDM model fitting against the cosmological data sets.

each experiment between VCDM and  $\Lambda$ CDM.

Fig. 1 shows 2-dimensional marginalised likelihoods for the cosmological parameters of interest in VCDM model. The Table II gives the values of the parameters within  $2\sigma$ 's.

From Table II, it is interesting to notice that the value of  $\beta_H$  does not reach 1 even at  $2\sigma$ . It means that the data prefer VCDM over  $\Lambda$ CDM. Moreover, the value of  $H_0$  estimated is in agreement with the low redshift measurement, and the tension is resolved. On top of that, it is to be noticed that even high redshift data (Planck Legacy 2018 data) tend to prefer the VCDM model (See Table I).

Let us look at the evolution of the background and perturbation variables to see the behaviour of the minimum of VCDM. Fig. 2 shows the behaviour of the function  $V(\phi)$  with respect to the auxiliary field  $\phi$  for the bestfit VCDM model. The behavior of  $H(z)$  in VCDM, with a

Parameters	95% limits
$\beta_H$	$0.919^{+0.038}_{-0.032}$
$A_2$	$0.0025^{+0.0054}_{-0.0215}$
$10^2\omega_b$	$2.241^{+0.026}_{-0.023}$
$\tau_{\text{reio}}$	$0.054^{+0.015}_{-0.012}$
$n_s$	$0.9673^{+0.0063}_{-0.0074}$
$H_0$	$73.98^{+2.6}_{-2.8}$
$\Omega_m$	$0.260^{+0.020}_{-0.018}$
$\sigma_8$	$0.872^{+0.027}_{-0.029}$

Table II. One-dimensional  $2\sigma$  constraints for the cosmological parameters of interest after the estimation with the cosmological data sets considered.

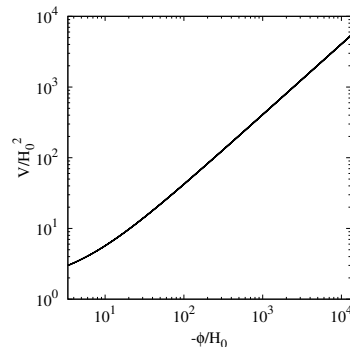


Figure 2. Behavior of the function  $V(\phi)$  with respect to the auxiliary field  $\phi$  in VCDM model. For high values of  $\phi$  (i.e. for high redshifts) the theory reduces to  $\Lambda$ CDM as  $V(\phi)$  approaches a straight line.

very small transition in the low redshift region which is visible in Fig.3, between the redshift  $10^{-3}$  and  $10^{-2}$ . It is clear from the choice of  $H(z)$  that this is a low-redshift resolution for Hubble tension.

Let us now look at the behaviour of the perturbation variables. First of all, Fig. 4 compares the CMB temperature correlation given the bestfit values for both VCDM and  $\Lambda$ CDM, with planck error bars. The low-redshift

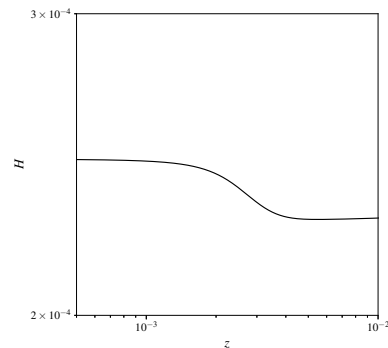


Figure 3. Zoomed version of  $H$  vs  $z$  plot. Here we can see the transition in the  $H(z)$  at very low redshift between  $10^{-3}$  and  $10^{-2}$ .

VCDM transition does not affect much the perturbation evolution. For example, the evolution of the energy density contrast  $\delta_\gamma$  of photons at low redshifts, in Fig. 5. We can see that the transition is smooth even at the order of  $\mathcal{O}(10^{-5})$ .

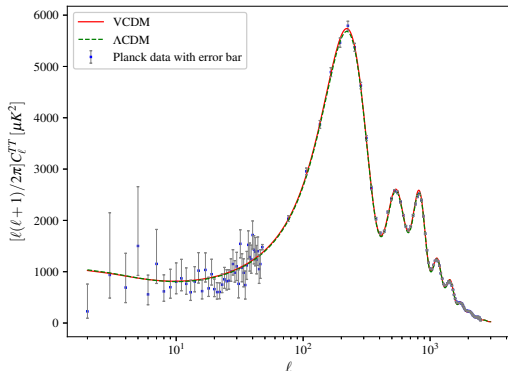


Figure 4. CMB TT correlation with bestfit for VCDM and  $\Lambda$ CDM including planck error bars.

Let us understand why the perturbation variables are always finite as long as the transition of  $H$  is finite. We have two perturbation equations of motion to be solved. Among the two,  $\phi$  has to be integrated, which depend on  $\dot{H}$ . Consider integration of this equation between  $t_* - \Delta t/2$  and  $t_* + \Delta t/2$ , where  $t_*$  is the time at which transition happens and  $\Delta t$  is the time width of the transition,

$$\begin{aligned} \Delta\phi &= \int_{t_* - \Delta t/2}^{t_* + \Delta t/2} \dot{\phi} dt = \int_{t_* - \Delta t/2}^{t_* + \Delta t/2} \left( \underbrace{A}_{\text{finite}} + \underbrace{B}_{\text{finite}} \dot{H} \right) dt \\ &= \underbrace{B \Delta H}_{\text{at } t=t_*} + \mathcal{O}(\Delta t). \end{aligned} \quad (12)$$

Since  $A$  and  $B$  are finite and as far as  $\Delta H$  is finite, then the perturbation  $\phi$  should also be finite even in the limit  $\Delta t \rightarrow 0$ . Hence all the perturbation variables affected

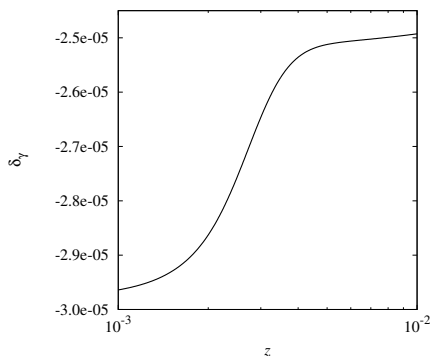


Figure 5. Zoomed version of  $\delta_\gamma$ , in the redshift range,  $10^{-3} < z < 10^{-2}$ . We can see the transition is smooth at the order of  $10^{-5}$ .

by  $\phi$  should also be finite, however fast the transition is. This means that, as far as  $A_3 (> 0)$  is small enough, the behaviour of the background and perturbation variables is not sensitive to its actual value. This explains the origin of degeneracy along the  $A_3$  direction in the parameter space.

In this report we showed that the notorious  $H_0$  tension can be addressed by a very minimal modification to the standard cosmological model, dubbed VCDM. We see that the value of  $H_0$  estimated is in agreement with the measurements from the low redshift observations. It is also noticed that this model fits the cosmological data sets better than  $\Lambda$ CDM by improving the  $\chi^2$  by 20.60. Background and perturbation variables are stable and finite. Hence we propose the VCDM model as a possible solution to the  $H_0$  tension. Finally we want to stress here that violations of 4D diffeo are only present in the gravity sector. Matter sector Lagrangians are fully covariant in 4D. Since gravity is modified in the IR limit, and because of the absence of any extra gravitational mode other than the standard gravitons, we expect that graviton loop corrections to be negligible.

The work of A.D.F. was supported by Japan Society for the Promotion of Science Grants-in-Aid for Scientific Research No. 20K03969. The work of S.M. was supported by JSPS KAKENHI Grant Numbers 17H02890, 17H06359, and by WPI MEXT, Japan. M.C.P. acknowledges the support from the Japanese Government (MEXT) scholarship for Research Student. Numerical computation in this work was carried out at the Yukawa Institute Computer Facility.

\* antonio.defelice@yukawa.kyoto-u.ac.jp  
 † shinji.mukohyama@yukawa.kyoto-u.ac.jp  
 ‡ masroor.cp@yukawa.kyoto-u.ac.jp

- [1] Adam G. Riess, Stefano Casertano, Wenlong Yuan, Lucas M. Macri, and Dan Scolnic. Large Magellanic Cloud Cepheid Standards Provide a 1% Foundation for the Determination of the Hubble Constant and Stronger Evidence for Physics beyond  $\Lambda$ CDM. *Astrophys. J.*, 876(1):85, 2019.
- [2] Kenneth C. Wong et al. H0LiCOW XIII. A 2.4% measurement of  $H_0$  from lensed quasars: 5.3 $\sigma$  tension between early and late-Universe probes. 7 2019.
- [3] M.J. Reid, J.A. Braatz, J.J. Condon, L.J. Greenhill, C. Henkel, and K.Y. Lo. The Megamaser Cosmology Project: I. VLBI observations of UGC 3789. *Astrophys. J.*, 695:287–291, 2009.
- [4] Wendy L. Freedman et al. The Carnegie-Chicago Hubble Program. VIII. An Independent Determination of the Hubble Constant Based on the Tip of the Red Giant Branch. 7 2019.
- [5] N. Aghanim et al. Planck 2018 results. VI. Cosmological parameters. 7 2018.
- [6] Jose Luis Bernal, Licia Verde, and Adam G. Riess. The trouble with  $H_0$ . *JCAP*, 10:019, 2016.

- [7] Adam G. Riess. The Expansion of the Universe is Faster than Expected. *Nature Rev. Phys.*, 2(1):10–12, 2019.
- [8] Antonio De Felice, Andreas Doll, and Shinji Mukohyama. A theory of type-II minimally modified gravity. *JCAP*, 09:034, 4 2020.
- [9] Andrew R Liddle. Information criteria for astrophysical model selection. *Mon. Not. Roy. Astron. Soc.*, 377:L74–L78, 2007.
- [10] N. Aghanim et al. Planck 2018 results. V. CMB power spectra and likelihoods. 2019.
- [11] Florian Beutler, Chris Blake, Matthew Colless, D. Heath Jones, Lister Staveley-Smith, Lachlan Campbell, Quentin Parker, Will Saunders, and Fred Watson. The 6dF Galaxy Survey: Baryon Acoustic Oscillations and the Local Hubble Constant. *Mon. Not. Roy. Astron. Soc.*, 416:3017–3032, 2011.
- [12] Ashley J. Ross, Lado Samushia, Cullan Howlett, Will J. Percival, Angela Burden, and Marc Manera. The clustering of the SDSS DR7 main Galaxy sample – I. A 4 per cent distance measure at  $z = 0.15$ . *Mon. Not. Roy. Astron. Soc.*, 449(1):835–847, 2015.
- [13] Shadab Alam et al. The clustering of galaxies in the completed SDSS-III Baryon Oscillation Spectroscopic Survey: cosmological analysis of the DR12 galaxy sample. *Mon. Not. Roy. Astron. Soc.*, 470(3):2617–2652, 2017.
- [14] M. Betoule et al. Improved cosmological constraints from a joint analysis of the SDSS-II and SNLS supernova samples. *Astron. Astrophys.*, 568:A22, 2014.
- [15] Diego Blas, Julien Lesgourgues, and Thomas Tram. The Cosmic Linear Anisotropy Solving System (CLASS) II: Approximation schemes. *JCAP*, 1107:034, 2011.
- [16] Masroor C. Pookkillath, Antonio De Felice, and Shinji Mukohyama. Baryon Physics and Tight Coupling Approximation in Boltzmann Codes. *Universe*, 6:6, 2020.
- [17] Benjamin Audren, Julien Lesgourgues, Karim Benabed, and Simon Prunet. Conservative Constraints on Early Cosmology: an illustration of the Monte Python cosmological parameter inference code. *JCAP*, 1302:001, 2013.
- [18] Thejs Brinckmann and Julien Lesgourgues. MontePython 3: boosted MCMC sampler and other features. *Phys. Dark Univ.*, 24:100260, 2019.
- [19] Antony Lewis. GetDist: a Python package for analysing Monte Carlo samples. 10 2019.